

# A Predictive Current Control Strategy for a Naturally-Commutated Converter Using a Finite-State Machine Model

VICTOR GUERRERO  
Universidad Tecnica  
Federico Santa Maria  
Dept. of Electronics  
Av. Espana 1680, Val  
CHILE  
victor.guerrerob  
@alumnos.usm.cl

JORGE PONTT  
Universidad Tecnica  
Federico Santa Maria  
Dept. of Electronics  
Av. Espana 1680, Val  
CHILE  
jorge.pontt  
@usm.cl

MARCELO VASQUEZ  
Universidad Tecnica  
Federico Santa Maria  
Dept. of Electronics  
Av. Espana 1680, Val  
CHILE  
marcelo.vasquez.lastra  
@gmail.com

MANUEL OLIVARES  
Universidad Tecnica  
Federico Santa Maria  
Dept. of Electronics  
Av. Espana 1680, Val  
CHILE  
marcelo.olivares  
@usm.cl

*Abstract:* Predictive current control methods for forced-commutated converters, e.g., voltage source inverter, are well documented and they perform very well compared with the classical solutions, i.e., hysteresis control and proportional-integral controllers with pulsewidth modulation. This paper presents a strategy to implement a predictive control technique for a naturally-commutated converter, e.g., multipulse cycloconverter. This strategy uses a discrete-time model of the system to predict the future value of the load current for all possible output voltages of the converter. Since in a naturally-commutated converter the possible output voltages are dynamic and they depend on the present switching state of every semiconductor of the converter, these output voltages must be obtained from a mathematical model (finite-state machine) of the converter. The proposed current control strategy is tested. The simulation and experimental results show that a predictive control strategy can be used not only in applications with forced-commutated converters but also with naturally-commutated converters showing good electric performance.

*Key-Words:* Predictive Control, Cycloconverter, naturally-commutated converters, Thyristors.

## 1 Introduction

Control strategies for electric converters is one of the main subjects in power electronics and has become a well documented topic for many different converters. Hysteresis (nonlinear method) and proportional-integral (PI) controllers using pulsewidth modulation (PWM) has been extensively studied and they are considered as the classical solution for the drive control problem [1].

The development of powerful microprocessors has increased the interest in predictive current control [2], [3]-[5], [20]- [21]. In this method (model-based predictive method), load and converter models are used to predict the electric behaviour of the system, and thereby select the most appropriate actuation following an arbitrary control criteria. This strategy has been used in many applications like current control for inverters [6], rectifiers and active filters with promising results [8], [17], [18].

In the last few decades the field of high-power drives has shown a great development, mainly because all industrial processes have been increasing their power demand in way to achieve a large-scale economy. Multipulse cycloconverters (a naturally-commutated converter) represent one of the most preferred solutions for high-power applications. This is way, cycloconverters are still a concern for the engineering community [9], [13], [14].

The main topic of the existing literature is related to predictive current control for applications with forced-commutated converters (e.g. IGBT and IGCT semiconductors). In these applications, the predictive control strategy is based on the fact that only a finite switching states can be generated by the converter and all this switching states can be achievable in any time. Thus, the converter models used in this applications are quite simple. In fact, in many predictive current control applications the converter is sim-

ply modeled as a gain [2]. Predictive control strategies for naturally-commutated converters, e.g. multipulse cycloconverters with thyristors, need a different converter model, because the switching state of the converter is not fully controlled and the output voltage depends on the input voltage of the converter.

In this paper, a finite-state machine is used to model a multipulse cycloconverter. With this model it is possible to implement a predictive control strategy for a naturally-commutated converter. This new synergy between model predictive control (MPC) and naturally-commutated converters may result in an improvement in high-power applications where these types converters are still the preferred choice to feed high-power electric machines.

Section II shows the implementation of a predictive control strategy for a force-commutated converter. Section III shows the proposed method to implement a predictive control strategy for a naturally-commutated converter, in this case for a 12-pulse cycloconverter. Also, this section discusses the difference in the modelling process for a forced and a naturally-converter. Finally, simulation and experimental results are presented to validate the proposed method.

## 2 Predictive Current Control for Forced-commutated Converters.

Predictive control technique for applications with forced-commutated converters is based on the fact that the converter can generate a finite number of output voltages, each one related with a specific switching state. The model predictive control (MPC) algorithm predicts the behaviour of the variables for each switching state. The optimum switching state is obtained due to a selection criteria represented by a quality function [7]. The switching state that minimize this quality function is applied to the converter. Basically, the MPC consists on three stages:

- Model of the converter (section II.A).
- Model of the system (section II.B).
- Control criteria, quality function.

The predictive current control block diagram for an electric machine is presented in Fig. 1. This control strategy can be summarized as follows.

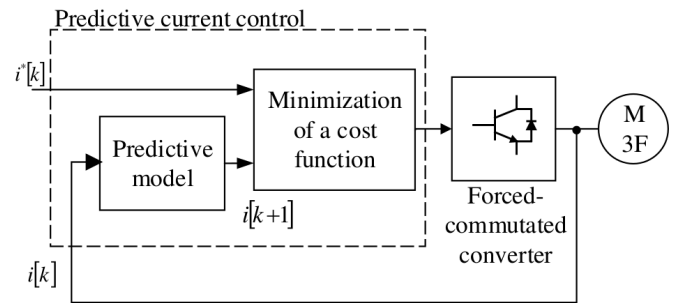


Figure 1: Predictive current control for forced-commutated converters.

1. The value of the reference current  $i^*[k]$  is obtained from an outer control loop and the load current  $i[k]$  is measured.
2. The model of the system is used to predict the value of the current for the next sampling interval  $i[k + 1]$ . Each possible output voltage of the converter is related with a specific switching state and a future current  $i[k + 1]$ .
3. The quality function  $g$ , see equation (1), is evaluated for all the possible switching states, each one related with a specific output voltage. The switching state that minimizes  $g$  is selected. The quality function may consider not only the current error ( $|i[k + 1] - i^*[k]|$ ), but also any other interesting control variable like common voltage mode, switching frequency, etc. These variables are represented by the function  $G(\cdot)$ . The parameters  $\lambda_i$  represent the weight factor of the control criteria.

$$g = \lambda_1 \cdot |i[k + 1] - i^*[k]| + \lambda_2 \cdot G(\cdot) \quad (1)$$

4. The gating signals are sent to the converter to accomplish the switching state that minimizes the quality function  $g$ .

### 2.1 Voltage source inverter model.

Fig. 2 shows the power circuit of a voltage source inverter. The gating signals  $g_i$  (with  $i = \{1, 2, \dots, 6\}$ ) establish the switching state and the output voltage

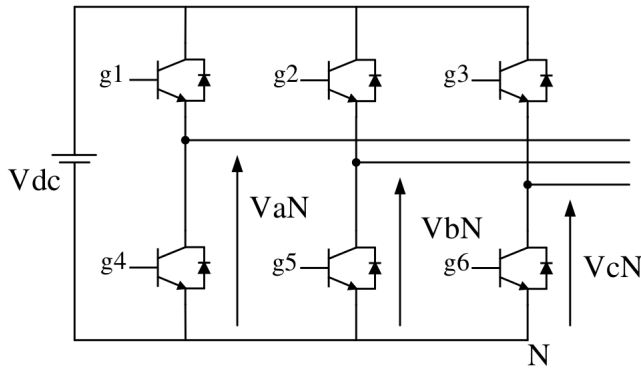


Figure 2: Voltage source inverter.

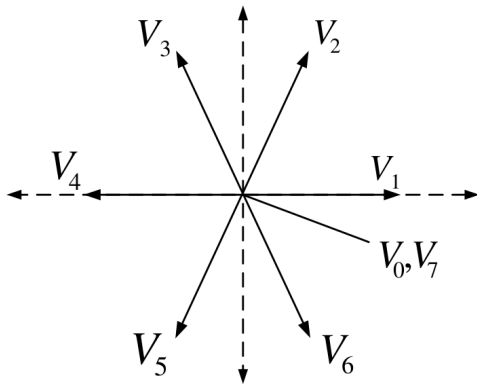


Figure 3: Voltage vectors generated by the inverter.

of the converter. Table I shows the relationship between the switching state of every semiconductor and the output voltage of the inverter.

Table I shows that the inverter has eight possible switching states, and consequently eight voltage vectors, two of them are redundant ( $v_0$  and  $v_7$ ). Therefore the inverter can be modeled as a nonlinear discrete system with seven possible output voltages. These voltages are shown in Fig. 3.

## 2.2 Machine model.

A model of the electric machine is needed to predict the behaviour of the variables evaluated by the quality function. This paper considers a permanent magnet synchronous machine (PMSM) as the system to control, because of the simplicity of its mathematical model. It is important to clarify that the way to

implement a predictive control strategy is practically the same for the all basic rotating electric machines types. Equations (2-4) represent the dynamic model of a PMSM in orthogonal  $\alpha\beta$  coordinates.

$$\frac{di_\alpha}{dt} = -\frac{R_s}{L_s}i_\alpha + \frac{\varphi_m}{L_s}\omega_r \sin \theta_r + \frac{1}{L_s}v_\alpha \quad (2)$$

$$\frac{di_\beta}{dt} = -\frac{R_s}{L_s}i_\beta - \frac{\varphi_m}{L_s}\omega_r \cos \theta_r + \frac{1}{L_s}v_\beta \quad (3)$$

$$\frac{d\theta_r}{dt} = \omega_r \quad (4)$$

Where:

- $i_\alpha, i_\beta$ : Stator currents in  $\alpha\beta$  coordinates.
- $v_\alpha, v_\beta$ : Output voltage of the inverter in  $\alpha\beta$  coordinates.
- $R_s, L_s$ : Stator resistance and inductance.
- $\varphi_m$ : Magnetic flux produced by the permanent magnets.
- $\omega_r, \theta_r$ : Rotor angle and speed.

A discrete-time model (with a sampling time  $h$ ) of the machine can be used to predict a future condition of the system measuring the stator currents in a  $k$ th sampling instant.

With the approximation:

$$\frac{di}{dt} \approx \frac{i[k] - i[k-1]}{h} \quad (5)$$

And using the equations (2-4), the future stator currents in orthogonal  $\alpha\beta$  coordinates can be determined by the following equations.

$$i_\alpha[k+1] = i_\alpha[k] + \quad (6)$$

$$h \cdot \left( -\frac{1}{\tau_s}i_\alpha[k] + \frac{\varphi_m}{L_s}\omega_r[k] \sin \theta_r[k] + \frac{1}{L_s}v_\alpha[k] \right)$$

$$i_\beta[k+1] = i_\beta[k] + \quad (7)$$

$$h \cdot \left( -\frac{1}{\tau_s}i_\beta[k] - \frac{\varphi_m}{L_s}\omega_r[k] \cos \theta_r[k] + \frac{1}{L_s}v_\beta[k] \right)$$

Table 1: Switching states of a voltage source inverter.

Voltage Vector	Gating Signals						Output Voltage		
	$g_1$	$g_2$	$g_3$	$g_4$	$g_5$	$g_6$	VaN	VbN	VcN
$v_0$	off	off	off	on	on	on	0	0	0
$v_1$	on	off	off	off	on	on	Vdc	0	0
$v_2$	off	on	off	on	off	on	0	Vdc	0
$v_3$	on	on	off	off	off	on	Vdc	Vdc	0
$v_4$	off	off	on	on	on	off	0	0	Vdc
$v_5$	on	off	on	off	on	off	Vdc	0	Vdc
$v_6$	off	on	on	on	off	off	0	Vdc	Vdc
$v_7$	on	on	on	off	off	off	Vdc	Vdc	Vdc

### 2.3 Predictive current control algorithm for a forced-commutated converter.

The predictive control algorithm consists of the following steps.

1. The reference current  $i^*[k]$  is obtained from an outer control loop.
2. The stator current  $i[k]$  and the rotor angle are measured  $\theta[k]$ .
3. With equations (6-7) and Table I the seven possible future currents  $i[k + 1]$  are predicted.
4. The voltage vector that minimizes the quality function  $g$  is selected.
5. The gating signals, related with the optimum switching state, are sent to the converter.
6. The sequence of steps is repeated.

## 3 A Predictive Current Control Strategy for a 12-pulse Cycloconverter.

The multipulse cycloconverter (CCV) is one of the most important naturally-commutated converters and it is the selected alternative for numerous high power low speed applications [10]-[12]. The CCV consists

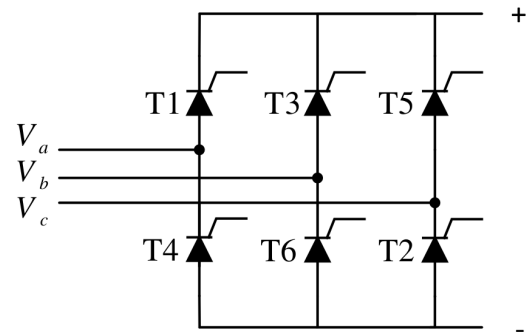


Figure 4: SCR rectifier.

on an arrangement of several Silicon-Controlled Rectifier (SCR) bridges (Fig. 4) connected on a back-to-back configuration. The proposed predictive current control method presented in this paper can be used for any multipulse cycloconverter, from 6-pulse to 24-pulse configuration. The 12-pulse CCV is one of the most common configurations in high-power applications and stills represents a major concern for the engineering community [13]-[16], thus this paper presents the predictive control strategy for this particularly multipulse cycloconverter.

### 3.1 12-Pulse Cycloconverter model

Fig. 5 shows the power circuit of the 12-pulse Cycloconverter with free-circulating current configuration [19]. The CCV has four SCR bridges per phase, two of them connected in series (positive bridges) and

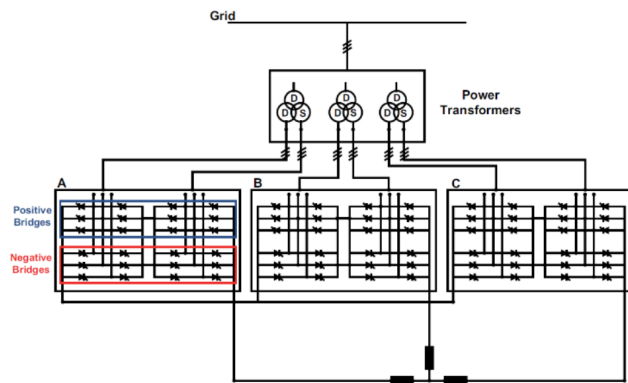


Figure 5: The 12-pulse Cycloconverter, free circulating current configuration.

Table 2: Conducting states for a SCR rectifier

Conducting State	Conducting SCR	Output Voltage
1	T1-T2	-Vca
2	T2-T3	Vbc
3	T3-T4	-Vab
4	T4-T5	Vca
5	T5-T6	-Vbc
6	T6-T1	Vab

the other two connected in a back-to-back configuration (negative bridges). The positive bridges conduct the positive cycle of the load current, see Fig. 5, and the negative bridges conduct the negative cycle of the load current (free circulating current configuration). The power transformers of the CCV have a delta-wye connected windings on its secondary to achieve a 12-pulse behaviour for the output voltage.

As previously mentioned, forced and naturally-commutated convertes cannot be modelated in the same way. Section (II.A) shows a model for a voltage source inverter (forced-commutated converter), which consists in a discrete system with seven possible output voltages, where each one is evaluated by the quality function. A multipulse cycloconverter (naturally-commutated converter) cannot be modelated in the same way for two main reasons:

1. Thyristors are not fully controlled semiconductors. Hence, the switching state of a cycloconverter cannot be completely controlled.

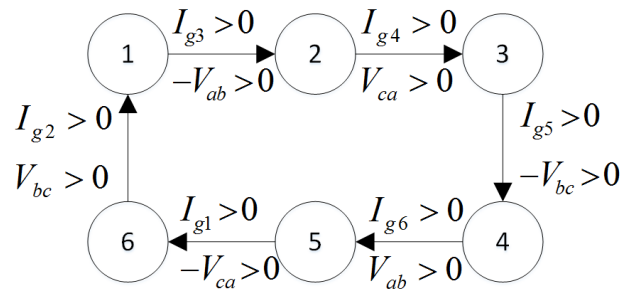


Figure 6: State machine for a SCR rectifier.  $I_g$  gating signals.

2. The output voltage of a CCV does not depend only by the gating signals of every thyristor, but also by the input voltage of the converter.

This paper propose a finite state machine model for the SCR bridge, which represents the essential unit of a multipulse cycloconverter.

A SCR bridge, see Fig. 4, has six admissible switching states. Table II shows the relationship between these admissible switching states and the output voltage in a SCR bridge. With these switching states the SCR bridge can be modelated as a finite state machine. The proposed model has six states, each one related with one of the six admissible switching states, see Fig. 6. The natural commutation sequence of a SCR bridge is  $\{1, 2, 3, 4, 5, 6, 1, 2, \dots\}$ . The variables that determine the next switching state in a SCR bridge are:

1. The gating signal of a particularly thyristor,  $I_g$  in Fig. 6.
2. The sign of a particularly input line to line voltage.

For example, if a SCR bridge is in the switching state 3 (thyristors T3 and T4 ON state), the bridge will pass to the switching state 4 only if two conditions are met: a) the input line to line voltage  $V_{bc}$  is negative and b) the gating signal  $I_{g5}$  triggers thyristor T5.

A 12-pulse cycloconverter has two SCR bridges working at the same time (free circulating current configuration). Each bridge has two alternatives: a) stay in the same switching state (represented by  $S$  on table III) or b) pass to the next switching state (represented by  $S + 1$ ). Table III shows the 64 possibles

Table 3: Possible future conducting states

Phase A		Phase B		Phase C		Case
Secondary Windings		Secondary Windings		Secondary Windings		
Star	Delta	Star	Delta	Star	Delta	
S	S	S	S	S	S	1
S+1	S	S	S	S	S	2
S	S+1	S	S	S	S	3
S+1	S+1	S	S	S	S	4
S	S	S+1	S	S	S	5
...						
S	S+1	S+1	S+1	S+1	S+1	63
S+1	S+1	S+1	S+1	S+1	S+1	64

future switching states for a 12-pulse cycloconverter. Each of these switching states must be evaluated by the quality function on the next stage of the predictive control algorithm. Some of these switching states will be neglected by the quality function, because they may not fulfill the line to line input voltage condition.

### 3.2 Quality Function

The quality function used in the proposed predictive strategy is represented by equations (8-11).

$$F_c = \lambda_1 \cdot (i_{dREF}[k] - i_d[k+1])^2 + \underbrace{\lambda_2 \cdot (i_{qREF}[k] - i_q[k+1])^2}_{\text{objective 1}} + \underbrace{I_{dMAX} + I_{qMAX}}_{\text{objective 2}} + \underbrace{st_{MAX}}_{\text{objective 3}} \quad (8)$$

$$I_{dMAX} = \begin{cases} \infty & \text{if } i_d[k+1] > i_{dmax} \\ 0 & \text{if } i_d[k+1] \leq i_{dmax} \end{cases} \quad (9)$$

$$I_{qMAX} = \begin{cases} \infty & \text{if } i_q[k+1] > i_{qmax} \\ 0 & \text{if } i_q[k+1] \leq i_{qmax} \end{cases} \quad (10)$$

$$st_{MAX} = \begin{cases} \infty & \text{for a not allowable switching state} \\ 0 & \text{for an allowable switching state} \end{cases} \quad (11)$$

Where:

- $F_c$ : Quality function value.
- $i_{dREF}[k], i_{qREF}[k]$ : Reference current in  $dq$  coordinates.
- $i_d[k+1], i_q[k+1]$ : Estimated currents in  $dq$  coordinates.
- $i_{dmax}, i_{qmax}$ : Maximum allowable current in  $dq$  coordinates.
- $\lambda_1, \lambda_2$ : Weight factors.

Note: The rotor angle  $\theta$  is the angular displacement between the  $dq$  coordinates and the  $\alpha\beta$  coordinates. For sufficiently small sampling times  $h$ ,  $i_{dREF}[k+1] \approx i_{dREF}[k]$  and  $i_{qREF}[k+1] \approx i_{qREF}[k]$  can be assumed. This approximation is considered in equation (8).

The quality function proposed in this paper has three main objectives:

- Objective 1: Select the switching state that minimizes the current error.
- Objective 2: Neglect the switching states that will generate over currents.
- Objective 3: Neglect the not allowable switching states due to an incorrect line to line input voltage.

### 3.3 Predictive current control algorithm for a cycloconverter.

The predictive current control algorithm proposed in this paper is presented as a flow diagram in Fig. 7. The main steps of this algorithm are:

1. Measure the stator currents and reference currents from the outer control loop.
2. Transform the measured currents from  $abc$  to  $\alpha\beta$  coordinates.
3. Using Tables II, III and the cycloconverter model, establish the 64 possible applicable voltages.
4. Using the discrete-time model of the electric machine, equations (6-7). Predict the possible future currents (time interval  $k+1$ ).

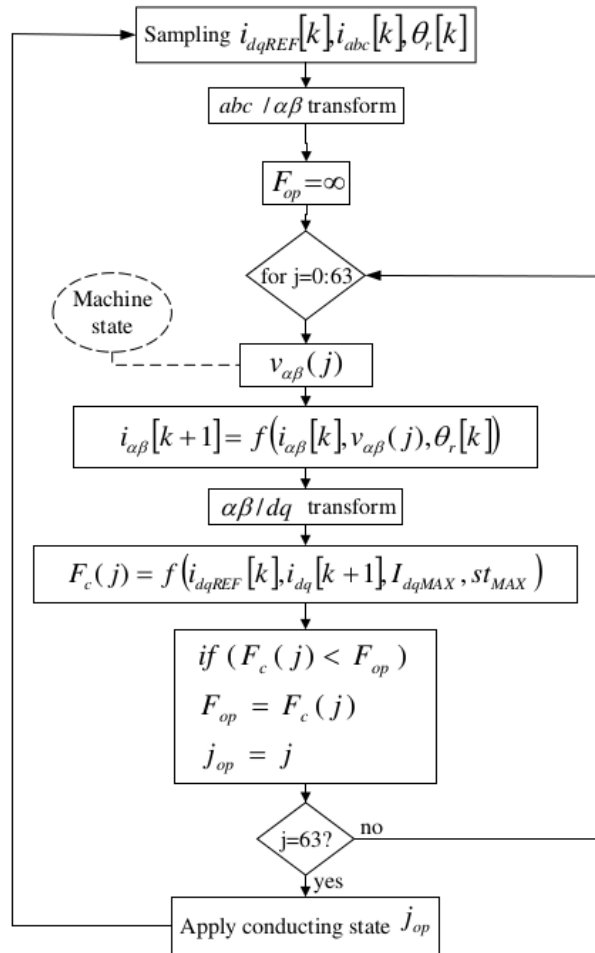


Figure 7: Flow diagram of the predictive strategy.

5. Transform the predicted currents from  $\alpha\beta$  to  $dq$  coordinates.
6. Evaluate the quality function, equations (8-11), for all current predictions.
7. The voltage corresponding to the predicted current for which the quality function is minimal is applied to the electric machine.

## 4 Simulation Results.

Simulation of a 12-pulse cycloconverter with free circulating current configuration controlled by the proposed predictive control strategy has been carried out

Table 4: PMSM Parameters

Parameter	Description	Value
$R_s$	Stator Resistance	0.3 [ $\Omega$ ]
$L_s$	Stator Inductance	8.2 [ $mH$ ]
$J$	Rotor Inertia	4 [ $kgm^2$ ]
$T_c$	Load Torque	10 [ $Nm$ ]
$B$	Friction Coefficient	0.002 [ $kgm^2/s$ ]

with Matlab/Simulink, in order to test the compatibility between a naturally-commutated converter and the MPC strategy and to probe that a predictive current controller can be implemented with a speed PI controller (outer-loop).

The simulation test has the following characteristics.

- The simulation system consists of a speed control of a permanent magnet synchronous machine PMSM. Table IV shows the considered parameters for the electric machine.
- Two controllers: a speed PI controller (outer-loop) and a current predictive controller (inner-loop).
- A sample time of  $h = 10^{-4}$  [s].
- Predictive control parameters for  $F_c$  on equations (8-11):

- $\lambda_1 = 1, \lambda_2 = 1.$
- $i_{dmax} = 10[A], i_{qmax} = 10[A].$
- $i_{dREF} = 0[A].$

Figures 8-11 show the results obtained from the simulation. Figure 8 shows the speed rotor of the PMSM. This figure shows that the inner current control loop (with a MPC controller) does not affect the performance of the outer control loop (speed PI controller). Figures 9-11 show a normal behaviour for the stator currents. As observe, Figure 9 shows that the stator currents do not exceed the maximum allowed value (10[A]) set by the inner current predictive control loop. Figure 10 shows that  $i_d$  follows the reference set by the predictive strategy ( $i_{dREF} = 0$ ) with an acceptable ripple,  $\pm 0.1[A]$ . The same behaviour occurs for the  $i_q$  stator current, Figure 11 shows that

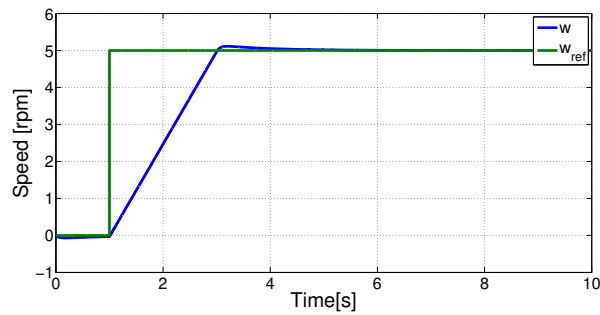


Figure 8: Rotor Speed PMSM. Simulation results.

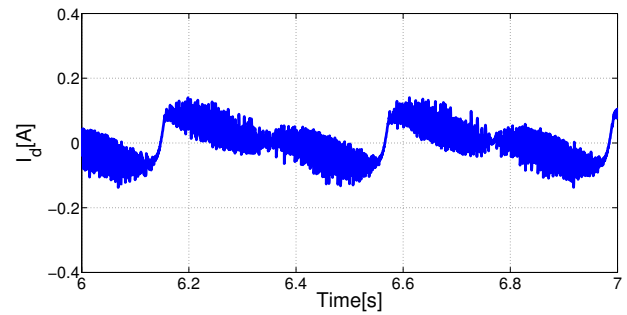
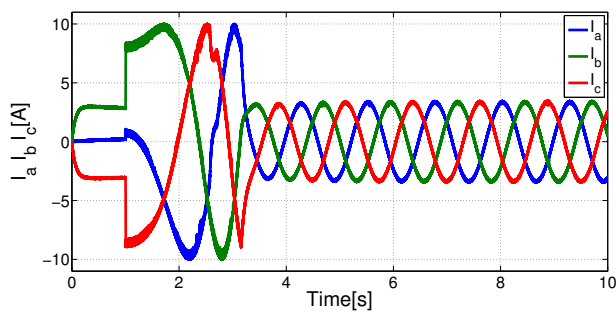
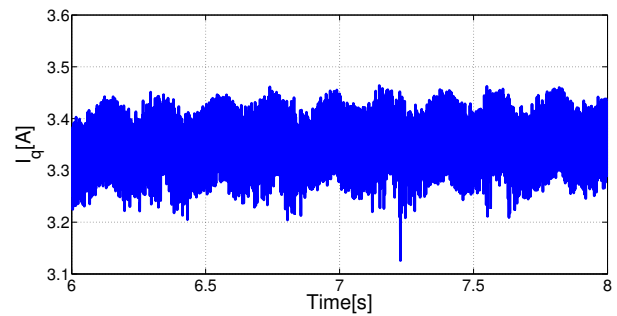
Figure 10:  $i_d$  stator current. Simulation results.

Figure 9: Stator currents PMSM. Simulation results.

Figure 11:  $i_q$  stator current. Simulation results.

the  $i_q$  current correctly follows the reference ( $3.35[A]$ ) with an acceptable ripple caused by the voltage spectrum of the cycloconverter.

## Comments

The simulation test shows that the proposed multi-pulse cycloconverter model, finite-state machine described on section III.A, allows a synergy between a naturally-commutated converter and a predictive control strategy.

The proposed predictive control strategy, with the finite-state machine model of the CCV, avoids the use of any type of modulator for the cycloconverter. The gating signals of every thyristors are generated directly by the model predictive controller.

Note: The absence of the modulation stage in the control scheme is not an exclusive advantage of the model predictive control, other control strategies also avoid the use of any modulator.

## 5 Experimental Results

Experimental tests were performed in way to validate the performance of the MPC strategy working with a finite-state machine model for the 12-pulse cycloconverter and to complement the simulation results obtained in section IV. The main focus of this experimental tests is to probe the feasibility of the implementation of the CCV finite-state machine model in a control platform (dSpace and a FPGA). Experimental results with current reference  $2[A]$  and frequency reference  $1[Hz]$  are presented.

The control algorithm was implemented in a dSpace platform and Spartan 3E FPGA for a  $1[kW]$  12-pulse cycloconverter with a RL load, as shown in Fig. 12.

### 5.1 Experimental Setup

The experimental tests have the following characteristics.

- dSPACE DS1103 R&D controller board.

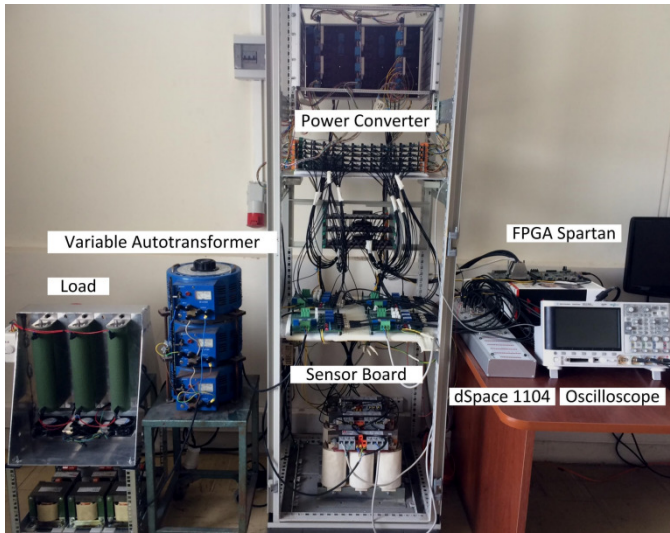


Figure 12: Experimental Set.

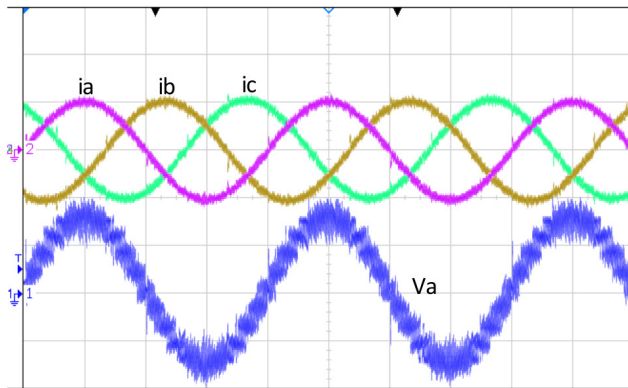


Figure 13: Stator currents and voltages. 2 [A]/div, 70[V]/div, 250 ms/div.

- Spartan-3E FPGA Starter Kit Board (Xilinx XC3S1600E FPGA).
- Continuously Variable Voltage Auto-Transformer 0 – 415[V], 20[A], 50[Hz] (CMV 20E-3).
- 3-phase Bridge Rectifier Modules 70[A], 800[V] (semikron SK70DT12).
- 50[Ω], 1[kW] Load Resistors.
- 65[mH], 5[A] Load Inductors.

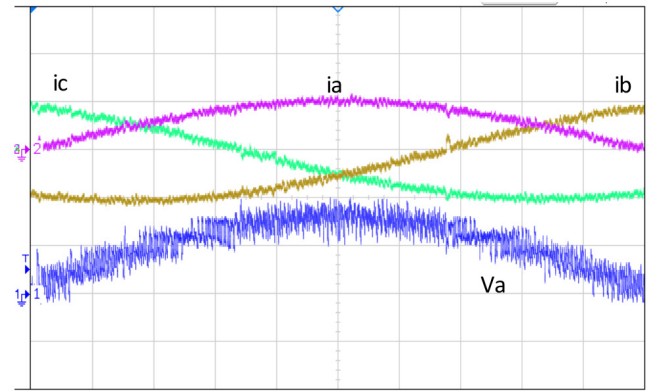


Figure 14: Stator currents and voltages. 2 [A]/div, 70[V]/div, 50 ms/div.

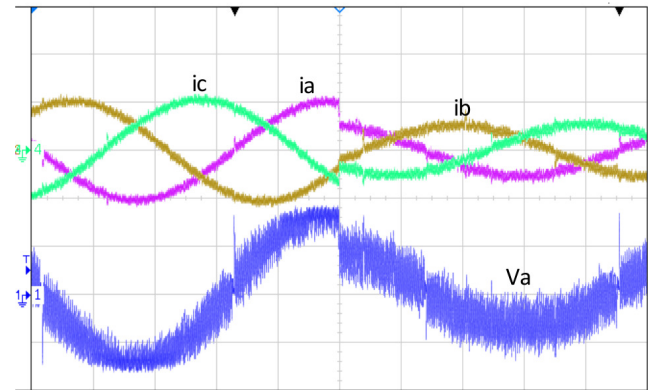


Figure 15: Stator currents and voltages for a step on  $i^*$ . 2 [A]/div, 70[V]/div, 250 ms/div

Table V shows a summary of the experimental setup for the steady-state performance test.

Table 5: Experiment setup

Parameter	Value
Reference current amplitude	2 [A]
Reference current frequency	1[Hz]
Resistance $R$	50 [Ω]
Inductance $L$	65 [mH]
Sampling Time $h$	700 [μs]

## 5.2 Steady-state and dynamical performance

The performance of the control strategy in steady-state is shown in Fig. 13 and 14. These figures show that the references for the 3-phase load currents ( $2[A]$  and  $1[Hz]$ ) are achieved with normal behaviour.

The dynamical performance of the control strategy is shown in Fig. 15. In this figure, a step in the load current reference from  $2[A]$  to  $1[A]$  is applied. The current references are achieved with great performance and dynamic response.

### Comments

The experimental tests show that the proposed finite-state machine model for a multipulse Cycloconverter allows a correct practical implementation of a MPC strategy for a naturally-commutated converter.

The proposed converter model can be applied without any major changes to any other naturally-commutated converter.

## 6 Conclusions

A finite-state machine model for a 12-pulse cycloconverter (naturally-commutated converter) and its practical implementation has been presented. It has been shown that the proposed converter model allows a synergy between a naturally-commutated converter and a predictive control strategy.

The modelling strategy for naturally-commutated converters proposed in this paper can be applied without any major changes to any type of cycloconverter. This strategy opens up new possibilities for model predictive control for multipulse cycloconverter applications and naturally-commutated converters.

The implementation of the proposed control strategy is simple and easy to implement in any type of control platform and avoids the use of any type of modulator, because the gating signals for the thyristors are generated directly by control.

The simulation and experimental results show a great steady-state and dynamical electric performance. Further work includes a more detailed comparison between the proposed strategy with the well-known hysteresis and PWM control, analysis of the steady-state and dynamic behaviour under parameter variations, implementation and stability issues, range of operation for the proposed strategy, etc.

### References:

- [1] J. Holtz, "Pulsewidth modulation for electronic power conversion," in Proceedings of the IEEE, vol. 82, no. 8, pp. 1194-1214, Aug 1994.
- [2] J. Rodriguez et al., "Predictive Current Control of a Voltage Source Inverter," in IEEE Transactions on Industrial Electronics, vol. 54, no. 1, pp. 495-503, Feb. 2007.
- [3] J. W. Moon, J. S. Gwon, J. W. Park, D. W. Kang and J. M. Kim, "Model Predictive Control With a Reduced Number of Considered States in a Modular Multilevel Converter for HVDC System," in IEEE Transactions on Power Delivery, vol. 30, no. 2, pp. 608-617, April 2015.
- [4] C. Xia, T. Liu, T. Shi and Z. Song, "A Simplified Finite-Control-Set Model-Predictive Control for Power Converters," in IEEE Transactions on Industrial Informatics, vol. 10, no. 2, pp. 991-1002, May 2014.
- [5] J. D. Barros, J. F. A. Silva and G. A. Jesus, "Fast-Predictive Optimal Control of NPC Multilevel Converters," in IEEE Transactions on Industrial Electronics, vol. 60, no. 2, pp. 619-627, Feb. 2013.
- [6] L. Tarisciotti, P. Zanchetta, A. Watson, S. Bifaretti and J. C. Clare, "Modulated Model Predictive Control for a Seven-Level Cascaded H-Bridge Back-to-Back Converter," in IEEE Transactions on Industrial Electronics, vol. 61, no. 10, pp. 5375-5383, Oct. 2014.
- [7] M. Uddin, S. Mekhilef and M. Rivera, "Experimental validation of minimum cost function-based model predictive converter control with efficient reference tracking," in IET Power Electronics, vol. 8, no. 2, pp. 278-287, 2 2015.
- [8] A. Calle-Prado, S. Alepuz, J. Bordonau, J. Nicolas-Apruzzese, P. Cortes and J. Rodriguez, "Model Predictive Current Control of Grid-Connected Neutral-Point-Clamped Converters to Meet Low-Voltage Ride-Through Requirements," in IEEE Transactions on Industrial Electronics, vol. 62, no. 3, pp. 1503-1514, March 2015.
- [9] V. Guerrero, J. Pontt, J. Dixon and J. Rebolledo, "A Novel Noninvasive Failure-Detection System for High-Power Converters Based on SCRs," in IEEE Transactions on Industrial Electronics, vol. 60, no. 2, pp. 450-458, Feb. 2013.

- [10] B. Wu, J. Pontt, J. Rodriguez, S. Bernet and S. Kouro, "Current-Source Converter and Cycloconverter Topologies for Industrial Medium-Voltage Drives," in *IEEE Transactions on Industrial Electronics*, vol. 55, no. 7, pp. 2786-2797, July 2008.
- [11] P. Castro Palavicino and M. A. Valenzuela, "Modeling and Evaluation of Cycloconverter-Fed Two-Stator-Winding SAG Mill Drive Part I: Modeling Options," in *IEEE Transactions on Industry Applications*, vol. 51, no. 3, pp. 2574-2581, May-June 2015.
- [12] P. Castro Palavicino and M. A. Valenzuela, "Modeling and Evaluation of Cycloconverter-Fed Two-Stator-Winding SAG Mill Drive Part II: Starting Evaluation," in *IEEE Transactions on Industry Applications*, vol. 51, no. 3, pp. 2582-2589, May-June 2015.
- [13] A. Symonds and M. Laylabadi, "Cycloconverter Drives in Mining Applications: A Typical Industrial System Is Analyzed and the Impact of Harmonic Filtering Considered," in *IEEE Industry Applications Magazine*, vol. 21, no. 6, pp. 36-46, Nov.-Dec. 2015.
- [14] P. A. Aravena, L. A. Morn, R. Burgos, P. Astudillo, C. Olivares and D. A. Melo, "High-Power Cycloconverter for Mining Applications: Practical Recommendations for Operation, Protection, and Compensation," in *IEEE Transactions on Industry Applications*, vol. 51, no. 1, pp. 82-91, Jan.-Feb. 2015.
- [15] V. Guerrero and J. Pontt, "Oscillatory torque caused by dead time in the current control of high power gearless mills," *IECON 2011 - 37th Annual Conference on IEEE Industrial Electronics Society*, Melbourne, VIC, 2011, pp. 1966-1970.
- [16] V. G. Barra and J. P. Olivares, "Design of a 12-pulse cycloconverter with fault-tolerance capability," *Power Electronics and Applications (EPE 2011)*, Proceedings of the 2011-14th European Conference on, Birmingham, 2011, pp. 1-10.
- [17] S. Kouro, M. A. Perez, J. Rodriguez, A. M. Llor and H. A. Young, "Model Predictive Control: MPC's Role in the Evolution of Power Electronics," in *IEEE Industrial Electronics Magazine*, vol. 9, no. 4, pp. 8-21, Dec. 2015.
- [18] Rodriguez J.; Kazmierkowski, M.P.; Espinoza, J.R.; Zanchetta, P.; Abu-Rub, H.; Young, H.A.; Rojas, C.A., "State of the Art of Finite Control Set Model Predictive Control in Power Electronics," *Industrial Informatics, IEEE Transactions on*, vol.9, no.2, pp.1003,1016, May 2013.
- [19] B.R. Pelly, *Thyristor Phase-Controlled Converters and Cycloconverters*, New York: Wiley Interscience, 1971.
- [20] T. J. Besselmann, S. Van de moortel, S. Almr, P. Jrg and H. J. Ferreau, "Model Predictive Control in the Multi-Megawatt Range," in *IEEE Transactions on Industrial Electronics*, vol. 63, no. 7, pp. 4641-4648, July 2016.
- [21] T. J. Besselmann, S. Almr and H. J. Ferreau, "Model Predictive Control of Load-Commutated Inverter-Fed Synchronous Machines," in *IEEE Transactions on Power Electronics*, vol. 31, no. 10, pp. 7384-7393, Oct. 2016.